

# ChemComm

Accepted Manuscript



This is an *Accepted Manuscript*, which has been through the Royal Society of Chemistry peer review process and has been accepted for publication.

*Accepted Manuscripts* are published online shortly after acceptance, before technical editing, formatting and proof reading. Using this free service, authors can make their results available to the community, in citable form, before we publish the edited article. We will replace this *Accepted Manuscript* with the edited and formatted *Advance Article* as soon as it is available.

You can find more information about *Accepted Manuscripts* in the [Information for Authors](#).

Please note that technical editing may introduce minor changes to the text and/or graphics, which may alter content. The journal's standard [Terms & Conditions](#) and the [Ethical guidelines](#) still apply. In no event shall the Royal Society of Chemistry be held responsible for any errors or omissions in this *Accepted Manuscript* or any consequences arising from the use of any information it contains.

## When protein-based biomineralization meets hydrothermal synthesis: the nanostructures of the as-prepared materials are independent of the protein types

Received 00th January 20xx,  
Accepted 00th January 20xx

DOI: 10.1039/x0xx00000x

[www.rsc.org/](http://www.rsc.org/)

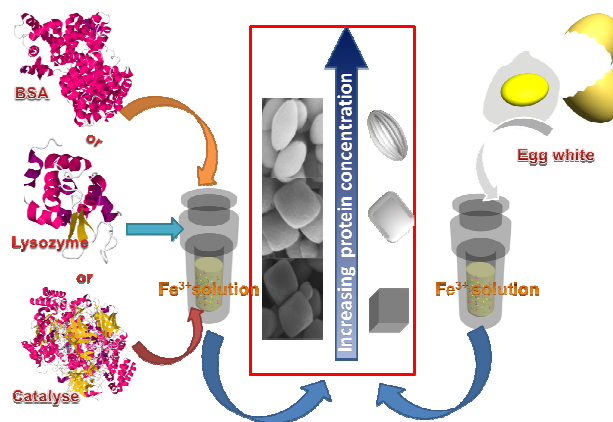
Liqiang Wang<sup>†,‡,a</sup>, Xiangzhi Li<sup>‡,a</sup>, Xingxing Jiang<sup>a</sup>, Wansong Chen<sup>a</sup>, Lanshuang Hu<sup>a</sup>, Maru Dessie Walle,<sup>a</sup> Liu Deng<sup>a</sup>, Minghui Yang<sup>\*a</sup>, You-Nian Liu<sup>\*a</sup> and Srećko I. Kirin<sup>b</sup>

**Proteins were proved to be type-independent templates for biomineralizing iron ions into hematite mesocrystals with tunable structures and morphologies under hydrothermal conditions. Our founding could pave the way for the synthesis of mesocrystals with controlled structures and morphologies using templates of low-cost proteins.**

Biomineralization, in which organisms take advantage of their inherent biomolecules, for example, peptides, proteins or saccharides to template the formation of inorganic materials with controlled morphologies, has received tremendous attention in recent years.<sup>1</sup> Among these biomolecules, proteins are of particular interests. Generally, protein could impose significant influence on the way of nucleation and growth of inorganic crystals because of their preference towards interacting with a certain crystal face.<sup>2</sup> Meanwhile, the diversity of proteins, arising from their unique conformations, affords scientists numerous opportunities to synthesize inorganic nanocrystals shaped selectively via screening suitable proteins. Noteworthy, proteins covered on the nanocrystal surfaces could not only stabilize the formed nanocrystals but also induce ordered self-assembly of the nanocrystals via the mutual interaction between protein molecules. This thermodynamically favored procedure could bring in hierarchical nanostructures.

Up to date, protein based biomineralization has contributed to various inorganic materials from nanoclusters to self-assembled mesocrystals of hierarchical structures. In particular, mesocrystals of hierarchical structures that possess both individual and collective properties inheriting from the primary units and the corresponding ensembles have gained great attention recently.<sup>1a,3</sup> Though biomineralization occurs under

ambient temperature, Chen and co-workers synthesized  $\alpha$ -Fe<sub>2</sub>O<sub>3</sub> mesocrystals via biomineralization under hydrothermal conditions recently.<sup>4</sup> They used silk fibroin, relatively resistant to high temperature, as a template for synthesizing hierarchical  $\alpha$ -hematite mesocrystals with tunable morphologies by changing the concentrations of protein. This discovery is of great significance, considering its perspectives in terms of combining the diversity of proteins and the powerful hydrothermal synthesis in constructing inorganic materials.



Scheme 1 Schematic illustration of the synthesis of hematite mesocrystals via protein templated biomineralization under hydrothermal conditions

Under hydrothermal conditions where the temperature is quite high (ca. 200 °C), the proteins are apt to bend, fold freely, and even decompose into oligopeptides and amino acids. These changes make the proteins a higher tendency to coordinate with metal ions, and the subsequent biomineralization could proceed. Thus, under hydrothermal conditions, the components of proteins, such as amino acid residuals and oligopeptides instead of proteins themselves play key roles in the biomineralization process. As a result, once proteins contain ample specific sequences or amino acids, they are like to template the formation of inorganic materials with particular nanostructures via biomineralization under

<sup>a</sup> College of Chemistry and Chemical Engineering, Central South University, Changsha, Hunan 410083, China.

E-mail: yangminghui@csu.edu.cn (M.H. Yang); liuyounian@csu.edu.cn (Y.-N. Liu).

<sup>b</sup> Chemistry Division of Materials Chemistry, Ruđer Bošković Institute, Bijenička cesta 54, 10000 Zagreb, Croatia

<sup>†</sup> Electronic supplementary information (ESI) available: Experimental details and characterization. See DOI:

<sup>‡</sup> These two authors contributed equally.

hydrothermal conditions. Thus, some expensive proteins used for biomineralization may be replaced by low-cost ones that contain similar necessary peptide sequences or even amino acid residues as expensive proteins do. Obviously, this could be of great value owing to their potential contribution to the scale-up preparation of inorganic nanomaterials. Therefore, it is important to acquire the behavior of proteins under hydrothermal conditions in terms of interacting with metal ions to complete the final biomineralization process.

In this communication, several proteins were selected to investigate whether or not the protein structures could exert distinctive differences on the structures and morphologies of hematite, which was extensively investigated for energy and catalysts<sup>5</sup> (Scheme 1). Firstly, bovine serum albumin (BSA) was chosen as a template for synthesis of hematite under hydrothermal conditions. Briefly, ferric chloride, as a precursor was mixed with BSA and stirred for 30 min at room temperature. After that, the mixture was put into a vessel, which was tightly sealed in a stainless steel autoclave, and then put in an oven at 160 °C upon hydrothermal treatment. The crude products were separated by centrifugation, followed by washing for several times with water. The as-prepared products were analyzed by XRD, XPS and Raman, which confirmed that the sample was composed of pure hematite ( $\alpha$ -Fe<sub>2</sub>O<sub>3</sub>) crystalline phase (see Fig.S1, S2(a, b) and S3). Surprisingly, we found that hierarchical hematite was also obtained when BSA was employed as a template. The morphology of hematite is the same as that made by silk fibroin reported by Chen and coworkers. Compared with fibrous silk fibroin, BSA is a globular protein with distinctively different sequences. Moreover, it cannot endure high temperature and lacks of GAGAGS motifs which were believed to play a key role in primary units self-assembling into hierarchical nanostructures.<sup>4</sup>

Despite of great discrepancies between BSA and silk fibroin, BSA is able to template the synthesis of hematite mesocrystals with hierarchical nanostructures via participating and further affecting the formation of the hierarchical structures. To further probe into the roles of BSA in the formation of hierarchical hematite, the products were characterized by SEM, TEM and etc. As displayed in Fig.1(a), the BSA biomineralized hematite nanoparticles are uniform, regular and entitled to olive-like geology of size 600 x 900 (nm). The energy dispersive X-ray (EDX) analysis demonstrates the existence of sulfide (S) and nitrogen (N), characteristic elements of BSA (see inset of the image in Fig.1(a)), consistent with the XPS results. In details, in high-resolution spectra, peaks of N, S elements could be easily observed (see Fig.S2(c,d)). These results illustrate that BSA took part in the formation of olive-like hematite, thus resulting in the co-existence of BSA constituents with hematite mesocrystals. Closer observation of the hematite nanoparticles shows that they were rough and composed of primary units (see Fig.1(b)). It is a typical characteristic of hierarchical mesocrystals that primary units formed under the assistance of protein then self-assemble into

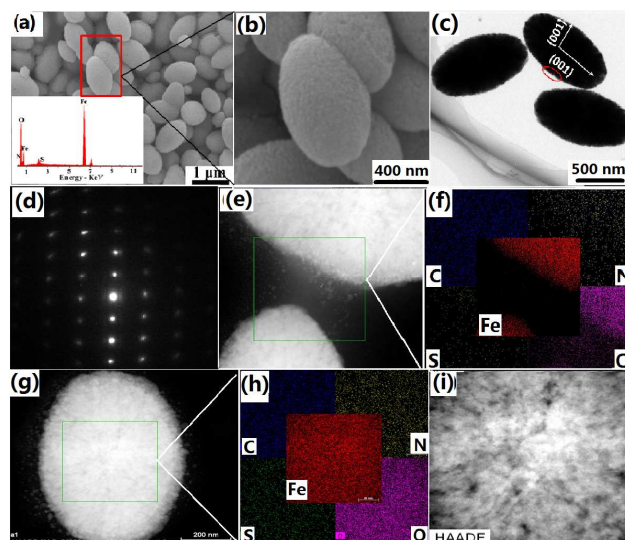


Fig. 1 (a, b) FESEM images of the olive-like hematite mesocrystals. (c, d) TEM image and corresponding SAED pattern of the marked area in image c (d). (e, g) HAADF-STEM images of olive-like hematite mesocrystals and (f, h) corresponding EDS mapping images (i) magnified image of selected area in (g). All samples utilized above were obtained after 10 h via BSA-templated biomineralization ([BSA] = 0.1 wt%, [Fe<sup>3+</sup>] = 0.06 M)

high ordered hierarchical structures.<sup>6</sup> TEM images further clarify that the hematite mesocrystals were self-assembled in a highly ordered way, which could be deduced from the selected area electron diffraction (SAED) pattern obtained from the edges (marked area)(see Fig.1(c, d)). A single-crystal diffraction pattern with slightly elongated spots could be clearly identified, demonstrating a well-accepted feature of mesocrystals formed via ordered arrangement of primary nanocrystals.<sup>3, 7</sup> High-resolution TEM images strongly verified such a highly ordered self-assembling behavior. As shown in Fig.S4, the contrast ratio of the different hematite mesocrystal edges are not the same, due to the different aggregation degree of the nanocrystals. In particular, more aggregation of nanocrystals lead to higher contrast ratio in the TEM images. Thus, we could reach the conclusion that the primary hematite nanocrystals gradually aggregate and extend to form the structured hematite mesocrystals with hierarchical structures.

The following studies also confirmed such statements, in which tremendous nanocrystals could be observed at the edge of the hematite mesocrystals after the ultrasound treatment (see Fig. 1(e, g)). Elemental mapping results by energy dispersive X-ray spectroscopy (EDS) show that N, S, C, O, Fe distributed homogeneously on a single mesocrystals (see 1(e)). However, this is not the case for the area between two mesocrystals, where only elements of N and S exist (see Fig.1(h)). Thus, it is rational to deduce that BSA could not only template the synthesis of the primary units, but also facilitate the metal ions self-assembly into the final hierarchical structures. HAADF-STEM image and cross-sectional compositional line profiles of the hematite mesocrystals also confirmed that the protein was well-proportioned on the surface of the mesocrystals. The intensity analysis may also suggest that more proteins are

entrapped in the inner of the mesocrystals for stabilizing the primary hematite nanocrystals (see Fig.S5).

This can also be inferred from the TGA results that two weight-loss stages can be recognized. The weight-loss stage below 200 °C is assigned to the evaporation of water, while the decomposition of BSA is located between 200 and 800 °C. Interestingly, the weight loss of BSA decomposition is not proportional to their addition (2.1% vs 8.0%) (see Fig.S6). This strongly suggests that a considerable amount of BSA are entrapped within the hematite mesocrystals, similar to the previous reported work.<sup>8</sup> Theoretically, aggregation voids are expected to occur when the primary units self-assemble into hierarchical mesocrystals, leaving nanopores on the surface of the nanoparticles. High-angle annular dark-field scanning TEM (HAADF-STEM, see Fig.1(i)) and nitrogen adsorption-desorption measurements both verified the formation of hematite mesocrystals and the average pore size was found to be 7 nm according to the Barrett-Joyner-Halenda (BJH) measurement (see Fig.S7). All those experimental results reach a consensus that BSA was involved in the formation of the hematite mesocrystals and hierarchical structures could be therefore induced.

Proteins could actually impose great differences on the structures as well as morphologies of hematite. Fig.2 shows the morphology evolution from cubic to spindle, olive-like morphology to the final cocoon-like shapes. Clearly, like silk fibroin, BSA-based biomineralization is also capable of synthesizing hematite mesocrystals with controlled structures as well as morphologies, both of which is able to influence the hematite performances.<sup>9</sup> Time-traced evolution of the olive-like hematite mesocrystals shows that needle-like nanoparticles emerged in the initial stage, then the olive-like nanoparticles formed gradually by prolonging the biomineralization time. This evolution process is believed to be the phase transition from  $\alpha$ -FeOOH to  $\alpha$ -Fe<sub>2</sub>O<sub>3</sub> under hydrothermal conditions (see Fig.S8).<sup>10</sup> The whole structural and morphological changes induced by BSA are consistent with that induced by silk fibroin. Although lack of GAGAGS motifs, BSA contains abundant Glu, Tyr, and His residues, which can coordinate strongly with Fe<sup>3+</sup> through nitrogen, oxygen and sulfur centers.<sup>11</sup> Such coordination could drive the nucleation and growth of crystals along the thermodynamically favored pathway, resulting in the occurrence of the final nanoparticles in a preferred structures and morphologies. In particular, like silk fibroin, BSA may also display poor interaction with (001) facet of crystals, which resulted in a similar morphological evolution process. Interestingly, many researches proved that proteins or short peptides display a weak binding ability towards low-index facets, (001) for instance, when they were used for biomineralization.<sup>12</sup>

The morphologies of the mesocrystals are often determined by the aggregation rate of the primary hematite crystal. The addition of BSA can obviously change the intensity ratio between (110) and (104), two characteristic peaks of hematite (see Fig.S1). This may lead to the olive-like hematite mesocrystals. However, when the protein concentration reaches a certain amount, proteins interact with the facets of

the crystals without preference. This may impede the growth of the crystals and then normal ordered array of the primary nanocrystals. Hence, in this case, the resulted nanoparticles were of relative smaller size, irregular morphologies with some aggregation defects (see Fig.S9). This can also be seen from the XRD pattern. When the BSA concentration increases to 0.5%, the intensity ratio between (110) and (104) of hematite is similar to that without BSA template (see Fig.S1), in good agreement with previously reported data that decreasing the Fe<sup>3+</sup> concentration can result in the formation of hematite nanoparticles with relative smaller size at certain protein concentration.<sup>4,13</sup>

To further clarify this protein-type independent biomineralization process, lysozyme and catalase that contain Glu, Tyr as well as His but lack of GAGAGS sequences were also adopted respectively as a template to synthesize hematite mesocrystals via biomineralization under hydrothermal conditions. As expected, hematite mesocrystals obtained by such an approach followed a similar morphological evolution from cubic to olive to the final olive-like shapes (see Fig.3(a-d)). It strongly suggests that protein types have no influence on the morphologies of nanocrystals formed by protein-based biomineralization under hydrothermal conditions.

It is worth to note all the proteins we used above as well as silk fibroin have to undergo complicated separation and purification process before use, inevitably increasing the cost and limiting their practical applications on large scale. Our investigation herein implies that under hydrothermal conditions the biomineralization processes were independent of the protein types. This may allow us to use relative low-cost proteins or even mixed ones instead of specific pure protein to complete the biomineralization process.

To confirm the above assumption, egg white (extracted directly from eggs without any purification) consisting of 90% water and several kinds of proteins including both fibrous and globular ones was adopted.<sup>14</sup> The experimental results showed that the olive-like hematite of hierarchical porous structures was obtained under the same experimental conditions (see Fig.3(e,f) and Fig.S10). This is of great practical significance especially considering the unparalleled low cost and abundance of egg white in nature.

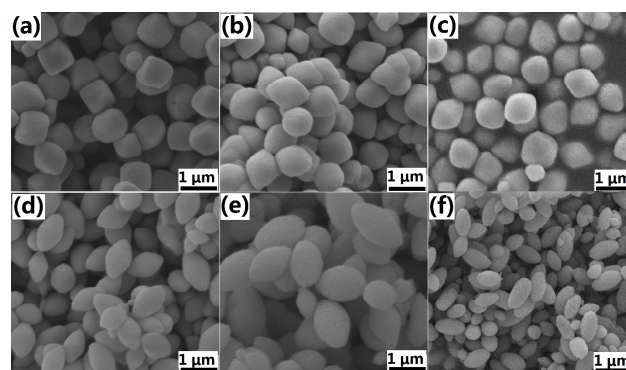


Fig.2 FESEM images of hematite mesocrystals obtained after 10h via BSA-templated biomineralization ( $[Fe^{3+}] = 0.06$  M) with different protein concentrations (a) 0 wt%; (b) 0.01 wt%; (c) 0.05 wt%; (d) 0.1 wt%; (e) 0.25 wt%; and (f) 0.5 wt%

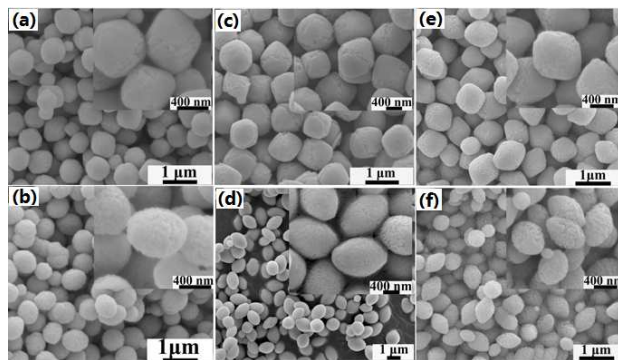


Fig. 3 FESEM images of hematite mesocrystals obtained after 10 h via different proteins templated biomineralization ( $[\text{Fe}^{3+}] = 0.06 \text{ M}$ ) with different protein concentrations. (a),(b) lysozyme 0.01 wt%, 0.05 wt%; (c),(d) catalase 0.01 wt%, 0.05 wt%; (e),(f) egg white 0.01 wt%, 0.05 wt%.

In summary, proteins were proved to be capable of templating the synthesis of hematite mesocrystals with tunable hierarchical structures under hydrothermal conditions. More importantly, the structures and morphologies of the as-obtained hematite mesocrystals are independent of the protein types. Protein concentration-dependent morphological changes could also be observed using lysozyme, catalase and even egg white. Our findings therefore not only afford an approach towards constructing hierarchical inorganic materials with tailoring morphologies, but also confirm that proteins containing certain similar components, for example, peptide sequences or even amino acid residues may bring in biomineralized inorganic materials with similar structures and morphologies under hydrothermal conditions. Our findings could pave the way for the synthesis of mesocrystals with controlled structures and morphologies more economically by using templates of low-cost proteins.

## Acknowledgement

This work was supported by the National Natural Science Foundation of China (No. 21476266, 21276285 and 21575165) and Natural Science Foundation of Hunan province (No. 2015JJ1019)

## Notes and references

1. (a) L. Bergstrom, E. V. Sturm, G. Salazar-Alvarez and H. Colfen, *Acc. Chem. Res.*, 2015, **48**, 1391; (b) M. B. Dickerson, K. H. Sandhage and R. R. Naik, *Chem. Rev.*, 2008, **108**, 4935; (c) J. N. Cha, G. D. Stucky, D. E. Morse and T. J. Deming, *Nature*, 2000, **403**, 289.
2. (a) J. Ge, J. D. Lei and R. N. Zare, *Nat. Nanotechnol.*, 2012, **7**, 428; (b) C. Y. Chiu, Y. J. Li, L. Y. Ruan, X. C. Ye, C. B. Murray and Y. Huang, *Nat. Chem.*, 2011, **3**, 393.
3. H. Colfen and M. Antonietti, *Angew. Chem., Int. Ed.*, 2005, **44**, 5576.
4. X. Fei, W. Li, Z. Z. Shao, S. Seeger, D. Y. Zhao and X. Chen, *J. Am. Chem. Soc.*, 2014, **136**, 15781.
5. (a) D. Koziej, A. Lauria and M. Niederberger, *Adv. Mater.*, 2014, **26**, 235; (b) P. Tartaj, M. P. Morales, T. Gonzalez-

- Carreño, S. Veintemillas-Verdaguer and C. J. Serna, *Adv. Mater.*, 2011, **23**, 5243.
6. L. S. Zhong, J. S. Hu, H. P. Liang, A. M. Cao, W. G. Song and L. J. Wan, *Adv. Mater.*, 2006, **18**, 2426.
7. R.-Q. Song and H. Cölfen, *Adv. Mater.*, 2010, **22**, 1301.
8. J. Ye, W. Liu, J. Cai, S. Chen, X. Zhao, H. Zhou and L. Qi, *J. Am. Chem. Soc.*, 2011, **133**, 933.
9. (a) V. Urbanova, M. Magro, A. Gedanken, D. Baratella, F. Vianello and R. Zboril, *Chem. Mater.*, 2014, **26**, 6653; (b) M. Hermanek, R. Zboril, I. Medrik, J. Pechousek and C. Gregor, *J. Am. Chem. Soc.*, 2007, **129**, 10929.
10. (a) Y. Luo, M.-S. Balogun, W. Qiu, R. Zhao, P. Liu and Y. Tong, *Chem. Commun.*, 2015, **51**, 13016; (b) F. Meng, S. A. Morin and S. Jin, *J. Am. Chem. Soc.*, 2011, **133**, 8408; (c) A. Navrotsky, L. Mazeina and J. Majzlan, *Science*, 2008, **319**, 1635.
11. (a) J. Fetter, J. Cohen, D. Danger, J. Sanders-Loehr and E. C. Theil, *JBIC*, 1997, **2**, 652; (b) G. S. Waldo and E. C. Theil, *Biochemistry*, 1993, **32**, 13262.
12. Q. Lu, F. Gao and S. Komarneni, *Adv. Mater.*, 2004, **16**, 1629.
13. X. Fei, Z. Shao and X. Chen, *J. Mater. Chem. B*, 2013, **1**, 213.
14. (a) R. Q. Lu, D. P. Yang, D. X. Cui, Z. Y. Wang and L. Guo, *Int. J. Nanomed.*, 2012, **7**, 2101; (b) Y. Mine, *World Poultry Sci J*, 2002, **58**, 31.